Conference on Modelling Fluid Flow (CMFF'22)
The 18th International Conference on Fluid Flow Technologies
Budapest, Hungary, August 30-September 2, 2022

APPROXIMATE DECONVOLUTION MODEL FOR TWO-DIMENSIONAL DECAYING HOMOGENEOUS ISOTROPIC TURBULENCE USING HIGH ORDER DISCRETIZATION SCHEMES

Lena CABAN[1], Agnieszka WAWRZAK[1], Artur TYLISZCZAK[1]

[1] Department of Thermal Machinery, Faculty of Mechanical Engineering and Computer Science, Czestochowa University of Technology. Armii Krajowej 21, 42-201 Czestochowa, Poland, E-mail: lena.caban@pcz.pl, agnieszka.wawrzak@pcz.pl, artur.tyliszczak@pcz.pl

ABSTRACT

The paper presents the results of numerical simulations of a two-dimensional homogenous isotropic turbulent flow carried out using the direct numerical simulation (DNS) and large eddy simulation (LES) methods. In the latter case, the classical Smagorinsky model and the Approximate Deconvolution Method (ADM) are used to model the sub-grid terms. In ADM the unfiltered variables are obtained from the iterative van Cittert method and are used to directly calculate the sub-grid tensor. The vorticity-stream function formulation of the Navier-Stokes equation is used in this work. We focus on the accuracy and dependence of ADM on the type of the filter (explicit, compact), its order, number of the iterations during the deconvolution procedure and the order of derivative discretization. Comparisons with DNS data are performed taking into account the basic quantities, e.g. the total energy, variance, and also higher order statistical moments (skewness and kurtosis). We found that when a high-order discretization method is used the ADM with compact difference type filtering schemes is more accurate than using the classical finite difference type filters.

Keywords: approximate deconvolution model, decaying homogeneous isotropic turbulence, high-order methods, large-eddy simulation

1. INTRODUCTION

Two-dimensional (2D) turbulence is not an ideal model of real turbulent flow. It does not occur in nature or in laboratory, but it finds applications in analysis of geophysical flows, such as oceanic and atmospheric phenomena, as well as in astronomy and plasma physics [1, 2, 3]. It is also important for understanding fully developed three-dimensional (3D) turbulence, although the behavior of its energy cascade is different than in real 3D flows [4, 5, 6]. In the latter case, the energy is transferred from large scales to smaller ones by the vortex stretching mechanism that does not exist in a 2D turbulent flow. In this case, according to the Kraichnan-Batchelor-Leith (KBL) theory, a reverse energy transfer takes place.

Direct numerical simulation (DNS) of such a complex phenomenon as turbulence requires a large amount of computing resources and is usually very time consuming. A common approach is to use large eddy simulations (LES), in which only large-scale vortices are directly calculated, while the effect of small sub-grid scales is modeled. The LES equations are formally defined with the low-pass filter operator that separates these scales. So far, various approaches to modeling the interactions of scales and the closure of the LES system have been presented [7]. A relatively novel one is the Approximate Deconvolution Model (ADM) introduced by Stolz and Adams [8]. The ADM uses the repeated filtering to approximate the unfiltered flow variables and then applies them to the unknown sub-grid terms to close the LES system. Initially, ADM was successfully applied in 3D turbulent flow modeling [9, 10, 11, 12]. Then it was used to model 2D turbulence in large-scale ocean circulation problems [13, 14] as well as to small-scale atmospheric boundary layer [15, 16, 17]. Recently, Boguslawski et al. [18] applied ADM based on the Wiener deconvolution method for 2D homogenous isotropic turbulence. San et al. [19] performed a detailed sensitivity analysis of the low-pass spatial filters for ADM-LES of homogeneous incompressible 3D flows using 2nd order finite difference discretization scheme. They considered various types of filters such as box filters, compact difference filters (CDF), known also as Padé-type filters, differential and hyper-differential filters. San and Staples [20] also tested various high-order numerical schemes such as explicit and compact finite differences, Arakawa scheme, dispersion-relation-preserving scheme, and the Fourier-Galerkin pseudospectral scheme for DNS of homogeneous

isotropic 2D decaying turbulent flows. In the present work, we continue this research applying different filters and discretization methods and perform comparisons not only for basic quantities (e.g. a total energy, variance) but also for higher-order statistical moments, i.e. skewness and kurtosis.

2. GOVERNING EQUATIONS

The dimensionless vorticity-stream function formulation of the Navier-Stokes equations for 2D incompressible flows can be written as follows:

$$\frac{\partial \omega}{\partial t} + u\frac{\partial \omega}{\partial x} + v\frac{\partial \omega}{\partial y} = \frac{1}{\mathrm{Re}}\left(\frac{\partial^2 \omega}{\partial x^2} + \frac{\partial^2 \omega}{\partial y^2}\right) \tag{1}$$

$$\frac{\partial^2 \psi}{\partial x^2} + \frac{\partial^2 \psi}{\partial y^2} = -\omega \tag{2}$$

where ω is the vorticity, ψ is the stream function, $u = \frac{\partial \psi}{\partial y}$, $v = -\frac{\partial \psi}{\partial x}$ are the velocity components and Re is the Reynolds number.

Denoting by G the filter kernel in physical space, the filtering of a general variable f is determined by the convolution operation $\bar{f} = G * f$, where $\int_{-\infty}^{\infty} G(\xi)\,\mathrm{d}\xi = 1$. Thus, applying the filtration operation to the equations (1) and (2) gives:

$$\frac{\partial \bar{\omega}}{\partial t} + \bar{u}\frac{\partial \bar{\omega}}{\partial x} + \bar{v}\frac{\partial \bar{\omega}}{\partial y} = \frac{1}{\mathrm{Re}}\left(\frac{\partial^2 \bar{\omega}}{\partial x^2} + \frac{\partial^2 \bar{\omega}}{\partial y^2}\right) + \tau_{\mathrm{SGS}} \tag{3}$$

$$\frac{\partial^2 \bar{\psi}}{\partial x^2} + \frac{\partial^2 \bar{\psi}}{\partial y^2} = -\bar{\omega} \tag{4}$$

where $\bar{u} = \frac{\partial \bar{\psi}}{\partial y}$, $\bar{v} = -\frac{\partial \bar{\psi}}{\partial x}$ and

$$\tau_{\mathrm{SGS}} = -\left(\overline{u\frac{\partial \omega}{\partial x}} + \overline{v\frac{\partial \omega}{\partial y}}\right) + \left(\bar{u}\frac{\partial \bar{\omega}}{\partial x} + \bar{v}\frac{\partial \bar{\omega}}{\partial y}\right) \tag{5}$$

is the sub-grid term which cannot be directly computed because the unfiltered variables u, v, and ω are unknown. The standard closure for this sub-grid term is usually based on the sub-grid viscosity, whereas in the ADM approach it is computed using the approximate unfiltered quantities.

3. APPROXIMATE DECONVOLUTION MODEL

In this paper, the ADM is based on the so-called iterative van Cittert deconvolution method [21], which applied for a general variable $\bar{f}$ can be written as:

$$f^* = \underbrace{\sum_{n=0}^{N_{\mathrm{ADM}}} (I - G)^n}_{G_a^{-1}} \bar{f} \tag{6}$$

where I is the identity operator and G_a^{-1} is the approximate inverse filter. With the deconvolution model, the unclosed sub-grid term can be closed as follows:

$$\tau_{\mathrm{SGS}} = -\underbrace{\left(\overline{u^*\frac{\partial \omega^*}{\partial x}} + \overline{v^*\frac{\partial \omega^*}{\partial y}}\right)}_{\mathrm{ADM}} + \left(\bar{u}\frac{\partial \bar{\omega}}{\partial x} + \bar{v}\frac{\partial \bar{\omega}}{\partial y}\right) \tag{7}$$

where u^*, v^*, and ω^* are the reconstructed variables.

In practical LES, the exact form of the filter function G is unknown. It is a combination of an implicit filter combined with mesh spacing and the filters induced by the numerical discretization of the first and second derivatives (G_I) [22]. In this paper, we do not attempt to precisely define the effective filter G_e such that $G_e = G_I G$. Moreover, the filter used in the ADM may be completely different from the LES filter. In this paper, however, we only consider the ideal situation when these two filters are equal and we focus on the effect of discretization on the simulation results. We consider two types of LES filters which are based on the explicit and compact filtering methods.

3.1. Explicit and compact filters

For simplicity, we consider a 1D periodic domain $[0, L]$ consisting of K uniformly distributed nodes $x_i = h(i-1)$, for $i = 1, \ldots, K$, with the mesh spacing $h = L/K$. The formulas derived for the 1D domain can be directly applied to 2D and 3D cases along separate lines in each direction.

The general formula for the explicit finite difference filtering (FDF) schemes can be written as:

$$\bar{f}_i = \frac{1}{2}\sum_{j=0}^{N_c} b_j^c \left(f_{i+j} + f_{i-j}\right) \tag{8}$$

and for the implicit compact filters (CDF) as:

$$\bar{f}_i + \sum_{k=1}^{M_c} a_k^c \left(\bar{f}_{i+k} + \bar{f}_{i-k}\right) = \frac{1}{2}\sum_{j=0}^{N_c} b_j^c \left(f_{i+j} + f_{i-j}\right) \tag{9}$$

where $\bar{f}_i$ are the filtered values at nodes x_i, f_i are the known discrete function values. The filters coefficients a_k^c and b_j^c can be calculated from the following system of $N_c + 1$ equations for FDF schemes:

$$\begin{cases} \sum\limits_{j=0}^{N_c} b_j^c = 1 \\ \sum\limits_{j=1}^{N_c} j^{2i} b_j^c = 0 \ \text{ for } \ i = 1, ..., N_c - 1 \\ T(\pi) = 0 \end{cases} \tag{10}$$

and from $M_c + N_c$ equations for CDF schemes:

$$\begin{cases} 1 + 2\sum\limits_{k=1}^{M_c} a_k^c = \sum\limits_{j=0}^{N_c} b_j^c \\ \sum\limits_{k=1}^{M_c} 2k^{2i} a_k^c = \sum\limits_{j=1}^{N_c} j^{2i} b_j^c \ \text{ for } \ i = 1, ..., N_c - 1 \\ T(\pi) = 0 \\ (\mathrm{d}^l T(\omega)/d\omega^l)(\pi) = 0 \ \text{ for } \ l = 2k, k = 1, ..., M_c - 1 \end{cases} \tag{11}$$

where

$$T(\omega) = \hat{G}_{(M_c,N_c)}(\omega) = \frac{\sum_{j=0}^{N_c} b_j^c \cos(j\omega)}{1 + 2\sum_{k=1}^{M_c} a_k^c \cos(k\omega)}, \quad (12)$$

is the filter kernel associated with CDF schemes (9) in Fourier space, known as the transfer function, and $\omega = 2\pi n/K$, for $0 \le n \le K/2$, is the so-called scaled wavenumber in the range $[0, \pi]$. In the case of FDF schemes that can be considered as CDF with $M_c = 0$, the formula (12) is reduced to the nominator. The highest possible order of filtration for the assumed stencils of Eqs. (8) and (9) is equal to $(2N_c)$ and $2(M_c + N_c - 1)$, respectively. This is achieved when all the coefficients a_k^c and b_j^c are explicitly determined from the expansions of f and $\bar{f}$ into the Taylor series and additional constraints for the transfer function. Figure 1. shows the transfer functions of some FDF and CDF schemes used in this work. Here, we only compare the results using second order filtering schemes with $M_c = 0, N_c = 1$, denoted as $G_{(0,1)}$ and with $M_c = 1, N_c = 1$, denoted by $G_{(1,1)}$.

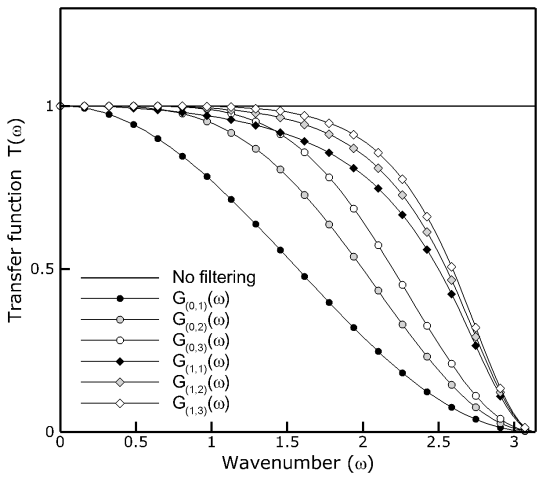

Figure 1. Transfer functions of G

4. NUMERICAL METHODS

The objective of this work is to test and evaluate the ADM model for 2D incompressible flow using explicit and compact high-order discretization methods and compare the results using the pseudospectral method. In this section, we briefly discuss the spatial discretization and temporal integration methods we use.

4.1. Spatial discretization methods

The general formula for the approximation of the first and second order derivatives using explicit finite difference (FD) and compact difference (CD) discretization schemes can be written as follows:

$$f_i' + \sum_{k=1}^{M} a_k \left(f_{i-k}' + f_{i+k}'\right) = \frac{1}{h}\sum_{j=1}^{N} b_j \left(f_{i+j} - f_{i-j}\right) \quad (13)$$

$$f_i'' + \sum_{k=1}^{M} a_k \left(f_{i-k}'' + f_{i+k}''\right) = \frac{1}{h^2}\sum_{j=1}^{N} b_j \left(f_{i+j} - 2f_i + f_{i-j}\right) \quad (14)$$

where FD schemes are obtained for $M = 0$. The highest possible order of approximation for given stencils M and N on the left and right-hand side of Eqs. (13) and (14) is equal to $2M + 2N$. This is obtained when all coefficients a_k and b_j are determined directly from the Taylor series expansions. The coefficients a_k and b_j can be derived from the following systems of $M + N$ equations:

$$\begin{cases} 1 + 2\sum_{k=1}^{M} a_k = 2\sum_{j=1}^{N} j^r b_j \\ \sum_{k=1}^{M}\left(\prod_{l=1}^{r}(2i+l)\right)k^{2i}a_k = \sum_{j=1}^{N} j^{2i+r} b_j \end{cases} \quad (15)$$

where the second equation is for $i = 1, ..., N + M - 1$. The case with $r = 1$ corresponds to the first order derivative approximation and $r = 2$ to the second order. Table 1 shows the discretization schemes we use in this work, along with their corresponding orders.

Table 1. Spatial discretization schemes and corresponding them approximation orders.

	FD scheme	CD scheme
2nd order	$M = 0, N = 1$	-
4th order	$M = 0, N = 2$	$M = 1, N = 1$
6th order	$M = 0, N = 3$	$M = 1, N = 2$
8th order	$M = 0, N = 4$	$M = 1, N = 3$
10th order	$M = 0, N = 5$	$M = 1, N = 4$
12th order	-	$M = 2, N = 4$
20th order	-	$M = 4, N = 6$

4.2. Temporal integration method

As we mainly concentrate on the accuracy of the spatial discretization methods and ADM, we use a fourth-order Runge-Kutta (RK) time integration scheme with a small time step $\Delta t = 5.0 \times 10^{-4}$. Taking into account Eq. (3) written as:

$$\frac{d\omega}{dt} = D(u, v, \omega) \quad (16)$$

where $D(u, v, \omega)$ is a discrete operator of spatial derivatives, the fourth-order RK scheme can be is

defined as:

$$\begin{aligned}
\omega^{(1)} &= D\left(u^n, v^n, \omega^n\right) \\
\omega^{(2)} &= D\left(u^n + \tfrac{\Delta t}{2}u^{(1)}, v^n + \tfrac{\Delta t}{2}v^{(1)}, \omega^n + \tfrac{\Delta t}{2}\omega^{(1)}\right) \\
\omega^{(3)} &= D\left(u^n + \tfrac{\Delta t}{2}u^{(2)}, v^n + \tfrac{\Delta t}{2}v^{(2)}, \omega^n + \tfrac{\Delta t}{2}\omega^{(2)}\right) \\
\omega^{(4)} &= D\left(u^n + \Delta t u^{(3)}, v^n + \Delta t v^{(3)}, \omega^n + \Delta t \omega^{(3)}\right) \\
\omega^{n+1} &= \omega^{(n)} + \tfrac{\Delta t}{6}\left(\omega^{(1)} + 2\omega^{(2)} + 2\omega^{(3)} + \omega^{(4)}\right)
\end{aligned} \tag{17}$$

where for $k = 1, 2, 3$ the velocity components $u^{(k)}$, $v^{(k)}$ are obtained from Eq. (4).

5. RESULTS

We consider a 2D periodic domain with the dimensions $L_x \times L_y = 2\pi \times 2\pi$. The flow field is initialized as a homogeneous isotropic turbulence (HIT) in accordance with the method suggested by San et al. [20], with the Taylor and Kolmogorov length scales equal to $l_t = 0.022L_x$ and $\eta = 0.00236L_x$, respectively. In two-dimensional turbulence, the inertial range in the energy spectrum is proportional to k^{-3}, where $k = |\underline{k}| = \sqrt{k_x^2 + k_y^2}$ is a wavenumber in Fourier space. The initial energy spectrum is given by the formula

$$E(k) = \frac{a_s}{2}\frac{1}{k_p}\left(\frac{k}{k_p}\right)^{2s+1} \exp\left[-\left(s + \frac{1}{2}\right)\left(\frac{k}{k_p}\right)^2\right] \tag{18}$$

in which the maximum value of initial energy spectrum is obtained for k_p, $a_s = \frac{(2s+1)^{s+1}}{2^s s!}$, and s is a shape parameter. As in [20], we take $k_p = 12$ and $s = 3$. The initial vorticity distribution is defined as

$$|\tilde{\omega}(\underline{k})|\sqrt{\frac{k}{\pi}E(k)}e^{i\zeta(\underline{k})} \tag{19}$$

where $\zeta(\underline{k}) = \xi(\underline{k}) + \eta(\underline{k})$ is the phase function, and $\xi(\underline{k}), \eta(\underline{k}) \in [0, 2\pi]$ are independent random values.

The results obtained using the ADM model described above are compared with the classical Smagorinsky model and filtered DNS data. In the Smagorinsky model, the sub-grid term is defined as

$$\tau_{\text{SGS}} = \nu_t\left(\frac{\partial^2\omega}{\partial x^2} + \frac{\partial^2\omega}{\partial y^2}\right) \tag{20}$$

where $\nu_t = (C_s\Delta)^2\sqrt{\bar{S}_{ij}\bar{S}_{ij}}$ is the non-dimmensional turbulent viscosity, C_s is the Smagorinsky constant, Δ is the filter width and S_{ij} is the strain rate tensor.

The simulations were carried out for the Reynolds number Re = 1000. The exemplary DNS results were obtained on the mesh with 1025^2 nodes and the results of the classical LES or applying ADM were obtained on the mesh consisting of 257^2 nodes. The total simulation time was $t = 10$ seconds.

The initial vorticity field and its evolution over time in the HIT configuration in the case of DNS is shown in Figure 2. At the time moment $t = 0$, large scale vortices do not exist. It can be seen that initially only small-scale turbulent structures are present. Over the time they form larger vortical structures and decay under the influence of the viscous forces.

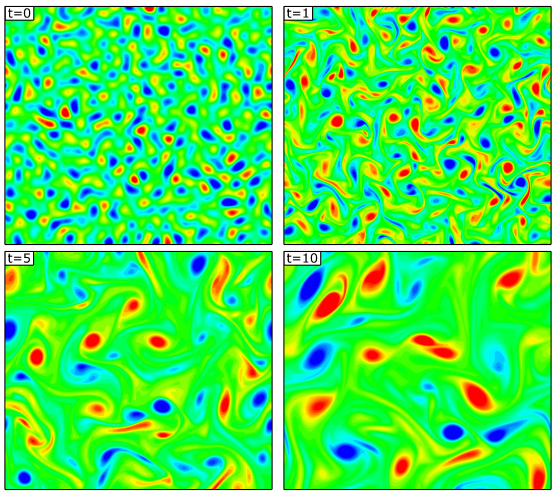

Figure 2. Vorticity contours in HIT configuration at various time moments.

In DNS and LES with the Smagorinsky model the 6th order CD scheme was used with $M = 1$ and $N = 2$ in Eqs. (13) and (14). The computations performed with ADM were performed with various FD, CD schemes and also pseudospectral discretization method. The results obtained using the ADM are compared with the results of DNS and also with those achieved without any model on the mesh consisting of 256^2 nodes .

Figure 3 shows the comparison of the energy spectrum for filtered values of DNS, classical Smagorinsky model and ADM with $N_{\text{ADM}} = 2$ using 2nd order FDF and CDF schemes and various discretization methods at time $t = 5$ seconds. It can be seen that in all cases the total energy of the flow predicted by both LES and ADM agrees relatively well with the filtered DNS solution.

However, there are significant differences for the higher central moments, such as variance, skewness and kurtosis, as shown in Figures 4 to 6. In these cases, the ADM provides much more accurate results compared to the classical LES. From the Figs. 4 to 6 we can also see that the ADM with CDF schemes is much more accurate than with FDF schemes.

Moreover, the results obtained without the subgrid model using the pseudospectral method diverges from DNS data. This is because the mesh 256^2 does not ensure a sufficient resolution and, as the pseudospectral method is not dissipative, it turns out to be unstable. It can be seen that the ADM stabilizes it correctly. Figure 7 shows the comparison of the vorticity fields at the time moment $t = 10$ for ADM with 2nd order FDF and CDF schemes and for 'No model' using the pseudospectral method with DNS vorticity field. It is worth noting that only the ADM with the

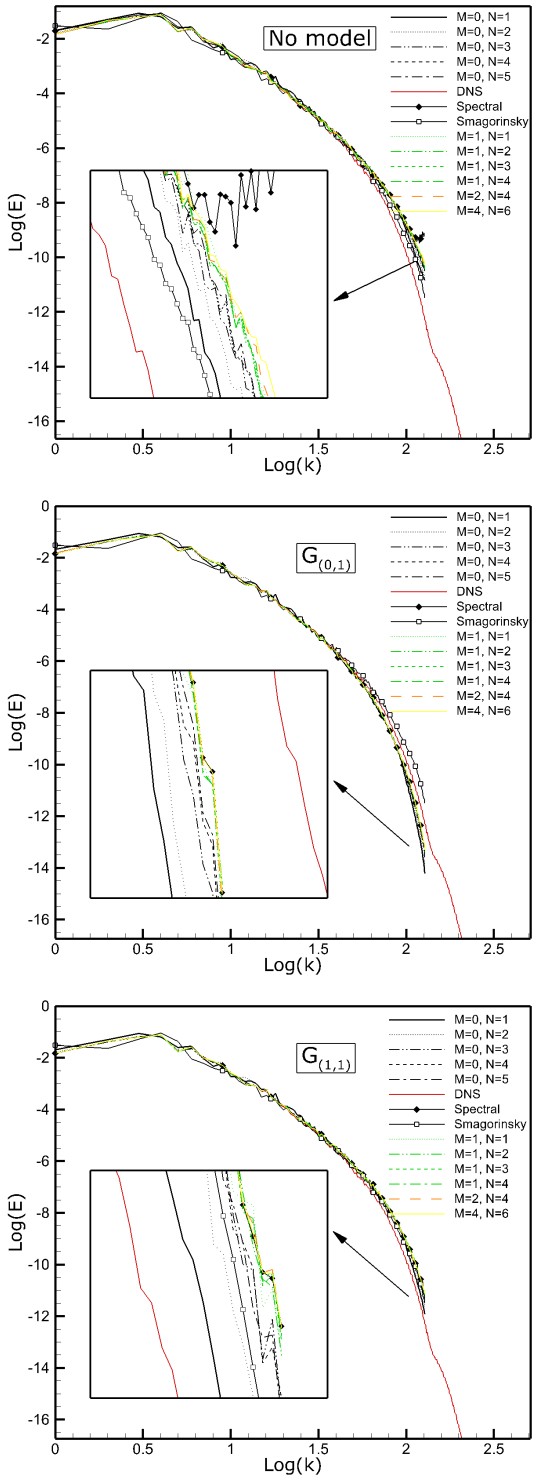

Figure 3. Energy spectra at time $t = 5$

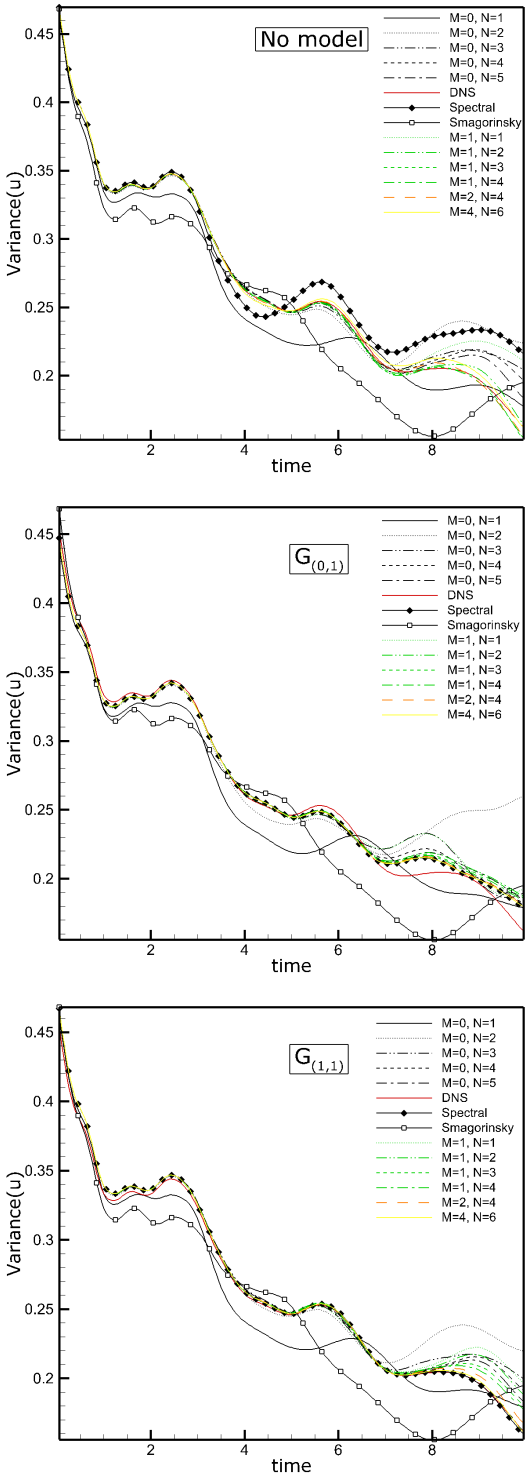

Figure 4. Variance of the u variable

pseudospectral CDF scheme almost perfectly agrees with DNS. As shown in [23], the higher the order of the CD discretization scheme, the results are closer to the spectral solutions.

6. SUMMARY

In this paper, we applied the Approximate Deconvolution Model (ADM) for numerical modeling a two-dimensional homogeneous isotropic turbulent flow. We analysed the effect of ADM accuracy and its dependence on the type of filter (explicit, compact) and its order. We also performed an analysis

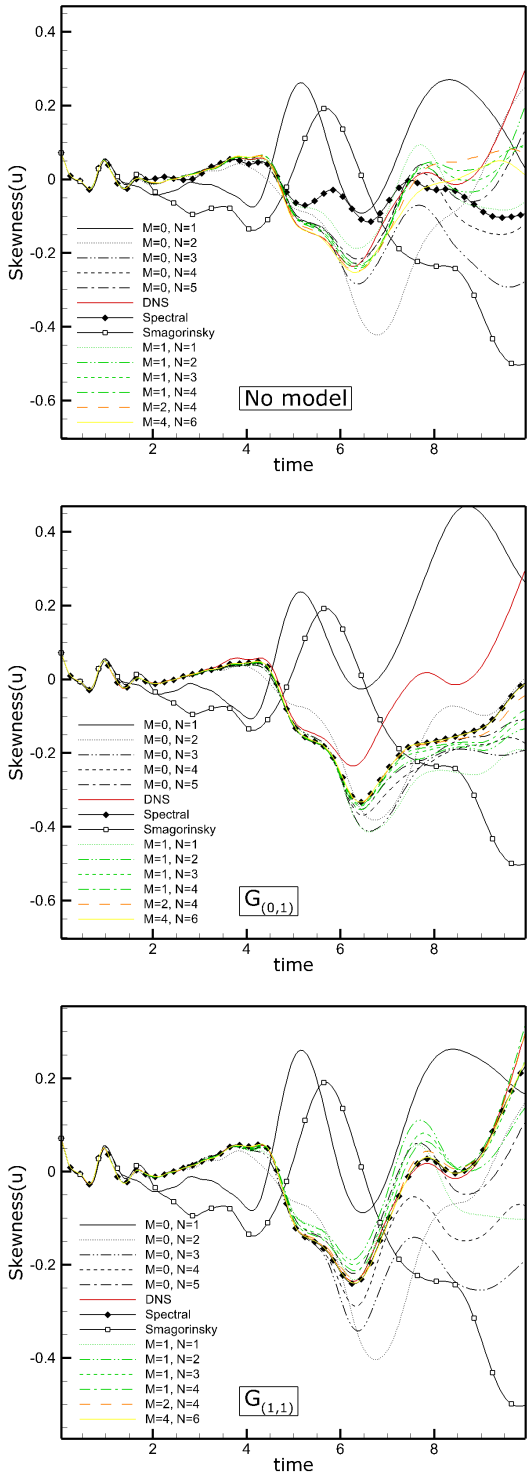

Figure 5. Skewness of the u variable

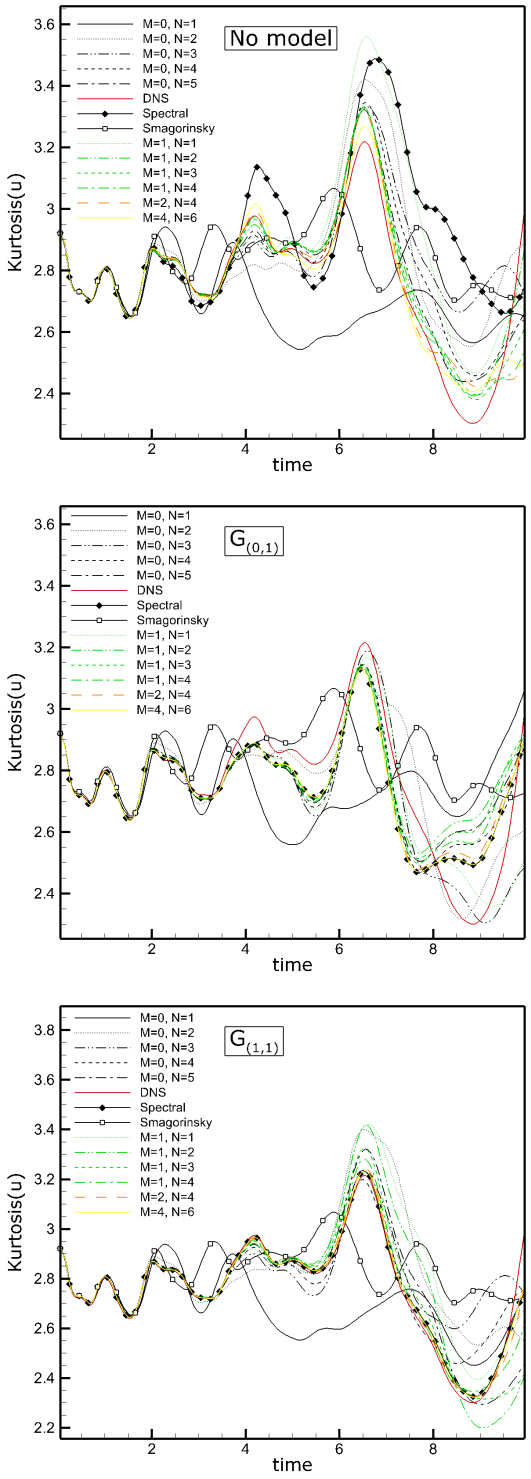

Figure 6. Kurtosis of the u variable

of ADM's dependence on various spatial discretization methods, such as explicit finite difference and compact difference schemes, as well as the Fourier pseudospectral method.

The results obtained using the ADM model were compared with the classical Smagorinsky model and the DNS data. It has been observed that the use of a higher order compact discretization scheme with the ADM model leads to nearly spectral accuracy. It was found that in such cases the ADM based on the compact filters is more accurate than using the classical finite difference type filters.

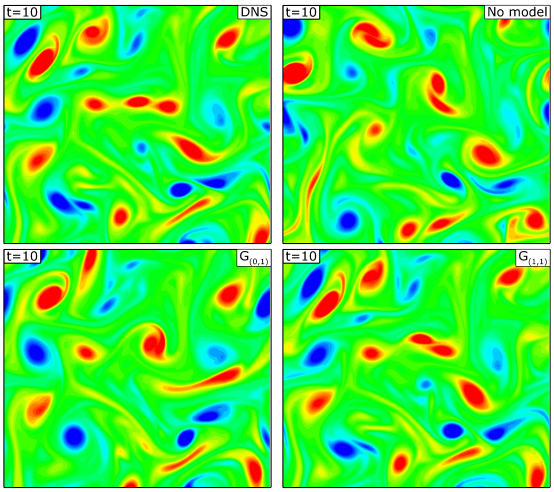

Figure 7. Vorticity contours in HIT configuration obtained in the simulations using DNS (upper left figure), 'no-model' approach (upper right), ADM with 2nd order FDF (lower left) and CDF (lower right).

ACKNOWLEDGEMENTS

This work was supported by the National Science Centre, Poland (Grant no. 2018/29/B/ST8/00262) and statutory funds of Czestochowa University of Technology BS/PB 1-100-3011/2021/P. The authors acknowledge Prof. Bernard J. Geurts for fruitful discussions stimulating this work within the framework of the International Academic Partnerships Programme No. PPI/APM/2019/1/00062 sponsored by National Agency for Academic Exchange (NAWA).

REFERENCES

[1] Danilov S. D., Gurarie D., 2000, "Quasi-two-dimensional turbulence", *Physics-Uspekhi*, Vol. 43 (9), pp. 863–900.

[2] Tabeling, P., 2002, "Two-dimensional turbulence - a physicist approach", *Physics Reports*, Vol. 362 (1), pp. 1–62.

[3] Boffetta G., Ecke R. E, 2012, "Two-Dimensional Turbulence", *Annual Review of Fluid Mechanics*, Vol. 44 (1), pp. 427–451.

[4] Kraichnan, R. H., 1967, "Inertial Ranges in Two-Dimensional Turbulence", *Physics of Fluids*, Vol. 10 (7), pp. 1417–1423.

[5] Batchelor, G. K., 1969, "Computation of the Energy Spectrum in Homogeneous Two-Dimensional Turbulence", *Physics of Fluids*, Vol. 12 (12), pp. 233–239.

[6] Leith, C. E., 1971, "Atmospheric Predictability and Two-Dimensional Turbulence", *Journal of the Atmospheric Sciences*, Vol. 28 (2).

[7] Sagaut, P., 2006, *Large Eddy Simulation for Incompressible Flows*, Springer, Berlin, Heidelberg.

[8] Stolz S., Adams N. A., 1999, "An approximate deconvolution procedure for large-eddy simulation", *Physics of Fluids*, Vol. 11 (7), pp. 1699–1701.

[9] Stolz S., Adams N. A., Kleiser L., 2001, "The approximate deconvolution model for large-eddy simulations of compressible flows and its application to shock-turbulent-boundary-layer interaction", *Physics of Fluids*, Vol. 13 (10), pp. 2985–3001.

[10] Stolz S., Adams N. A., Kleiser, L., 2001, "An approximate deconvolution model for large-eddy simulation with application to incompressible wall-bounded flows", *Physics of Fluids*, Vol. 13 (4), pp. 997–1015.

[11] Schlatter P., Stolz S., Kleiser L., 2004, "LES of transitional flows using the approximate deconvolution model", *International Journal of Heat and Fluid Flow*, Vol. 25 (3), pp. 549–558.

[12] Domaradzki J. A., Adams N. A., 2002, "Direct modelling of subgrid scales of turbulence in large eddy simulations", *Journal of Turbulence*, Vol. 3 (24), pp. 1–19.

[13] San O., Staples A. E., Wang Z., Iliescu T., 2011, "Approximate deconvolution large eddy simulation of a barotropic ocean circulation model", *Ocean Modelling*, Vol. 40 (2), pp. 120–132.

[14] San O., Staples A. E., Iliescu T., 2013, "Approximate deconvolution large eddy simulation of a stratified two-layer quasi-geostrophic ocean model", *Ocean Modelling*, Vol. 63, pp. 1–20.

[15] Chow F. K., Street R. L., Xue M., Ferziger J. H., 2005, "Explicit Filtering and Reconstruction Turbulence Modeling for Large-Eddy Simulation of Neutral Boundary Layer Flow", *Journal of the Atmospheric Sciences*, Vol. 62 (7), pp. 2058–2077.

[16] Chow F. K., Street R. L., 2009, "Evaluation of Turbulence Closure Models for Large-Eddy Simulation over Complex Terrain: Flow over Askervein Hill", *Journal of Applied Meteorology and Climatology*, Vol. 48 (5), pp. 1050–1065.

[17] Zhou B., Chow F. K., 2011, "Large-Eddy Simulation of the Stable Boundary Layer with Explicit Filtering and Reconstruction Turbulence Modeling", *Journal of the Atmospheric Sciences*, Vol. 68 (9), pp. 2142–2155.

[18] Boguslawski A., Wawrzak K., Paluszewska A., Geurts B. J., 2021, "Deconvolution of induced spatial discretization filters subgrid modeling in LES: application to two-dimensional turbulence", *Journal of Physics Conference Series*, Vol. 2090 (1), p. 012064.

[19] San O., Staples A. E., Iliescu T., 2014, "A posteriori analysis of low-pass spatial filters for approximate deconvolution LES of homogeneous incompressible flows", *International Journal of Computational Fluid Dynamics*, Vol. 29 (1), pp. 40–66.

[20] San O., Staples A. E., 2012, "High-order methods for decaying two-dimensional homogeneous isotropic turbulence", *Computers and Fluids*, Vol. 63, pp. 105–127.

[21] van Cittert P.H., 1931, "Zum Einfluß der Spaltbreite auf die Intensitätsverteilung in Spektrallinien. II", *Zeitschrift für Physik*, Vol. 69, pp. 298–308.

[22] Geurts B.J, van der Bos F., 2005, "Numerically induced high-pass dynamics in large-eddy simulation", *Physics of Fluids*, Vol. 17 (12), p. 125103.

[23] Caban L., Tyliszczak A., 2022, "High-order compact difference schemes on wide computational stencils with a spectral-like accuracy", *Computers and Mathematics with Applications*, Vol. 108, pp. 123–140.